

## Research Article

# Preparation of Graphene/TiO<sub>2</sub> Composite Nanomaterials and Its Photocatalytic Performance for the Degradation of 2,4-Dichlorophenoxyacetic Acid

**Donggen Huang, Tianzi Yang, Zhuanghong Mo, Qin Guo, Shuiqing Quan, Cui Luo, and Lei Liu**

*School of Resources Environment and Chemical Engineering, Nanchang University, Nanchang 330031, China*

Correspondence should be addressed to Donggen Huang; [dghuang1017@163.com](mailto:dghuang1017@163.com)

Received 13 May 2016; Accepted 13 July 2016

Academic Editor: Xuping Sun

Copyright © 2016 Donggen Huang et al. This is an open access article distributed under the Creative Commons Attribution License, which permits unrestricted use, distribution, and reproduction in any medium, provided the original work is properly cited.

The graphene (GR) was prepared by an improved electrochemical stripping method using a high-purity graphite rod as raw material and high temperature heat reduction in hydrogen atmosphere, and the graphene/TiO<sub>2</sub> (GR/TiO<sub>2</sub>) composite nanomaterials were manufactured by the method of sol-gel and high temperature crystallization in hydrogen atmosphere using butyl titanate and electrolysis graphene as precursors. The physical and chemical properties of the composites had been characterized by using X-ray diffraction (XRD), Fourier transform infrared spectroscopy (FTIR), UV-Vis spectrophotometer (UV-Vis), scanning electron microscopy (SEM), Transmission Electron Microscope (TEM), and specific surface area (SSA) by BET method. The photocatalytic properties of GR/TiO<sub>2</sub> composites nanomaterials in anoxic water were studied by using 2,4-dichlorophenoxyacetic acid (2,4-D) as probe. The results showed that graphite was well intercalated and peeled by a facile electrolysis method in different electric field environment; a well dispersed and rings structure of graphene was prepared by coupling ultrasound-assisted changing voltage electrochemical stripping technology. The as-prepared GR/TiO<sub>2</sub> composites had good performance for the photocatalytic degradation of 2,4-D in anoxic water; the chlorines were removed from benzene ring; the middle products of dichlorophenol, chlorophenol, phloroglucinol, and so forth were produced from the photocatalytic redox reaction of 2,4-D in anoxic water; parts of 2,4-D were decomposed completely, and CO<sub>2</sub> and H<sub>2</sub>O were produced.

## 1. Introduction

Recently, TiO<sub>2</sub> semiconductor photocatalytic technology has attracted great attention. TiO<sub>2</sub> has a discrete band structure; valence electrons were stimulated; transition to the conduction band, under ultraviolet excitation, photoproduction holes (h<sup>+</sup>), and electronics (e<sup>-</sup>) with high reactivity were formed in the valence band and conduction band, respectively [1]. But the recombination time of electronics (e<sup>-</sup>) and holes (h<sup>+</sup>) was in the scope of the ns ~ μs [2], leading to low efficiency of quantization. Surface structure of TiO<sub>2</sub> modification, which prolongs the service life of photoproduction electronics, is an important means to improve the photocatalytic activity of TiO<sub>2</sub> [3].

Graphene is a unique two-dimensional carbon allotrope that consists of a hexagonal array of sp<sup>2</sup>-bonded carbon

atoms. Being atomically thin, graphene has exceptionally high charge carrier mobility, thermal conductivity, strength, stiffness, impermeability, and current carrying capacity [4], makes full use of the electron transport properties of graphene, can effectively extend the recombination time of electronics (e<sup>-</sup>) and holes (h<sup>+</sup>) of TiO<sub>2</sub>, and improves the efficiency of quantum [5].

The preparation method of graphene mainly includes stripping method [6, 7], ultrasonic dispersion method [8], epitaxial growth method [9], chemical vapor deposition (CVD) [10, 11], solvent hot method [12], and oxidation reduction [13]. Batch of graphene can be prepared by using redox process; however, the as-prepared graphene contains oxygen functional groups [13] and topological defects such as five-carbon and six-carbon ring structure. These damage the complete structure of graphene and lead to the changes of

graphene inherent performance. Chemical vapor deposition is a research hotspot in recent years, but the high cost and complicated preparation technology and precise control condition restrict the development of the preparation method [10, 11]. Seeking a green, simple, and easy-to-repeat operation method is one of the hot topics in the study of graphene. Graphene whose layer number is less than seven was prepared under the effect of direct current (DC) using sulfuric acid as electrolyte and graphite as electrode [7]. The graphite oxide and graphene sheets were successfully synthesized by using ionic liquids as electrolytes and intercalation compound from graphite [14, 15]; however, the composition of the as-prepared graphene was complicated.

Electrochemical preparation of graphene has aroused sufficient attention in recent years. Usually, graphene was prepared by electrochemical method using ionic liquids [14, 15] and organic polymer electrolyte [7, 16] as electrolyte, but the composition of the as-prepared graphene was complicated and slice layer number was larger. The technology of electrochemical stripping graphite to prepare graphene under the coupling condition of ultrasonic and change voltage had not been reported.

In this paper, high-purity graphite rod was used as raw material; sulfuric acid and nitric acid mixture solution was used as electrolyte; graphene was prepared by electrochemical method under the coupling condition of ultrasonic and change voltage. GR/TiO<sub>2</sub> composite nanomaterials were prepared by the process of sol-gel and high temperature crystallization in hydrogen atmosphere using butyl titanate and electrolysis graphene as precursors. The microstructure and morphology of samples were characterized by XRD, UV-Vis, SEM, TEM, FTIR, and BET. The photocatalytic oxidation reduction characteristics of GR/TiO<sub>2</sub> in anoxic water by using 2,4-D as goal pollutant were studied, and the possible degradation mechanism was discussed.

## 2. Experimental Section

**2.1. Chemicals and Equipment.** 2,4-D was procured from Sigma Chemical Co., USA. All of the other chemicals used for the preparation of graphene and GR/TiO<sub>2</sub> composite nanomaterials and the determinations of chloride ion (Cl<sup>-</sup>) concentration were high-purity analytical reagents from Shanghai Chemicals Co., China. High-performance liquid chromatography (HPLC) grade HCOOH and methanol solvent were used for collecting the HPLC data. Reaction mixtures and the HPLC mobile phase were prepared with deionized water. Ultrasound instruments (KQ-200KDB, power input: 200 W, Kun Shan Ultrasonic Instruments, China) and direct current (DC) source (PS-303D, Yutai Electrical Instrumentation Industry Company, Shanghai) are used in the experiment.

### 2.2. Preparation of GR and GR/TiO<sub>2</sub> Composites

**2.2.1. Graphene Preparation.** The preparation process schematic diagram of graphene was shown in Figure 1. The electrolytic device was placed in ultrasonic system to maintain electrolyte vibration in the process of electrolysis.

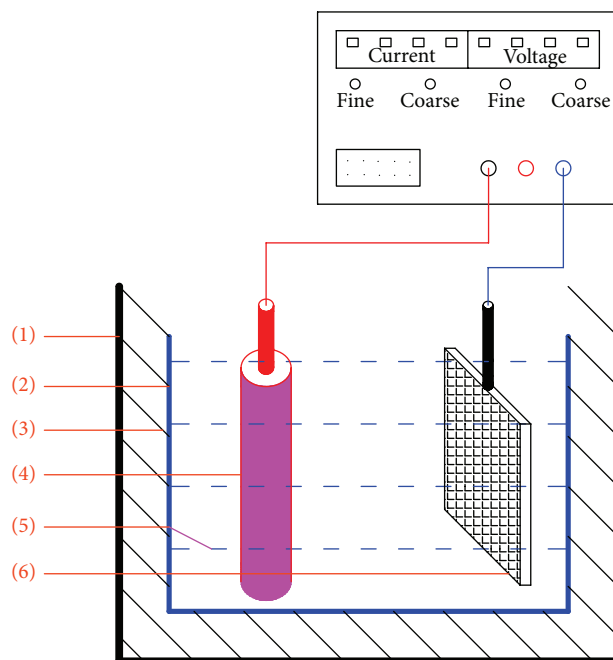


FIGURE 1: Schematic diagram of graphene electrolytic preparation ((1) ultrasonic apparatus; (2) electrolytic device; (3) H<sub>2</sub>O; (4) graphite rod; (5) electrolyte; (6) titanium mesh).

High-purity graphite rod and titanium sheet were used as anode and cathode, respectively. The distance between two electrodes was from 1 cm to 3 cm. DC source was used as power source; the voltage was in a range from 10 to 20 V (voltage change rate 1.7 V/30 min). One or more material mixtures from the selection of H<sub>2</sub>SO<sub>4</sub>, HNO<sub>3</sub>, H<sub>2</sub>O, CH<sub>3</sub>COOH, and so forth were used as electrolyte. Firstly, H<sub>2</sub>SO<sub>4</sub>:H<sub>2</sub>O = 0.08:1 (V/V) was used as electrolyte mother liquid; secondly, HNO<sub>3</sub>, CH<sub>3</sub>COOH, and so forth were used as doping agent, and H<sub>2</sub>SO<sub>4</sub>:HNO<sub>3</sub>:H<sub>2</sub>O = 0.08:0.02:1(V/V), H<sub>2</sub>SO<sub>4</sub>:HNO<sub>3</sub>:H<sub>2</sub>O = 0.08:0.04:1(V/V), H<sub>2</sub>SO<sub>4</sub>:HNO<sub>3</sub>:H<sub>2</sub>O = 0.08:0.06:1(V/V), and H<sub>2</sub>SO<sub>4</sub>:HNO<sub>3</sub>:H<sub>2</sub>O = 0.08:0.08:1(V/V), respectively; the electrolytic time was 3 hours; thirdly, the electrolytic product was filtered with quantitative filter paper and washed 3 times using warm deionized water; fourthly, filtering product was ultrasonic scattered dispersing 0.5 h with deionized water; the scattered product was filtered with quantitative filter paper again, and the graphene labeled as EGR was obtained by vacuum drying at 50°C. The other graphene products were prepared in the same way.

**2.2.2. Preparation of GR/TiO<sub>2</sub> Composites.** GR/TiO<sub>2</sub> composites were prepared by sol-gel and high temperature crystallization at muffle furnace in hydrogen atmosphere. Firstly, tetrabutyl titanate, ethanol, and acetic acid were put into a flask with stirring for 30 minutes to form solution A; EGR, ultrapure deionized water, nitric acid, and ethanol were mixed, stirring for 30 minutes to form solution B. Secondly, solution B was added dropwise to solution A under vigorous stirring. After the completion of addition, slow stirring

continued until the solution formed a transparent immobile gel. After drying at 50°C in vacuum dryer for 24 hours, the gel powder was put into tube muffle furnace in hydrogen atmosphere, raising the temperature of the muffle furnace by stage program, in the range 150–250°C; temperature rising rate was 0.5°C/min, but the heating rate was 1°C/min from 250°C to 450°C keeping the temperature of 450°C for 2 h; then the gray product of GR/TiO<sub>2</sub> composite was prepared.

According to the same preparation technology, a series of GR/TiO<sub>2</sub> composites containing different mass ratio of graphene/TiO<sub>2</sub> was labeled as 0.01 GR/TiO<sub>2</sub>, 0.015 GR/TiO<sub>2</sub>, 0.02 GR/TiO<sub>2</sub>, and 0.03 GR/TiO<sub>2</sub> were manufactured, by changing the quantities of EGR.

**2.3. Characterization of GR and GR/TiO<sub>2</sub> Composites Nanomaterial.** The phase constitution of GR and GR/TiO<sub>2</sub> composites were determined by X-ray diffractometry (Shimadzu, XD-3A) using nickel filtered copper radiation (Cu K $\alpha$ ) at 30 kV, 30 mA over 2 $\theta$  range of 5–80°.

Fourier transform infrared spectroscopy (FTIR) was recorded for KBr disks containing EGR, TiO<sub>2</sub>, and GR/TiO<sub>2</sub> using FTIR spectrometer (Nicolet 5700, US) with a scanning range of 4000–500 cm<sup>-1</sup>, respectively.

The surface areas of samples were determined from nitrogen adsorption-desorption isotherms at liquid nitrogen temperature using Micromeritics ASAP2020 equipment (US) with outgas for 15 min at 150°C. The Brunauer-Emmett-Teller (BET) method was used for surface area calculation.

The morphology and microstructure of the as-prepared graphene and GR/TiO<sub>2</sub> composites nanomaterial were examined by SEM (JSM 6701E, Japan). GR or GR/TiO<sub>2</sub> composite was mixed with methanol and scattered in the ultrasonic device for 4 h; the graphene methanol mixture was deposited on a copper mesh by dip coating and placed in room temperature for 2 h.

Morphology and size of the as-prepared graphene and GR/TiO<sub>2</sub> composites nanomaterial were also by TEM (JEM-2100, Japan); the graphene and GR/TiO<sub>2</sub> were deposited on a copper mesh by means of dip coating and placed for several days in room temperature, respectively.

#### 2.4. Photocatalytic Activity of GR/TiO<sub>2</sub> Composites Nanomaterial

**2.4.1. Experimental Set-Up.** The schematic diagram was shown in Figure 2. The outside of the cylindrical photoreactor made of glass with a diameter of 12 cm and a length of 60 cm was a cooling water sleeve to maintain stable reaction temperature. An 11 W ultraviolet lamp (wavelength: 275–320 nm) was used as light source; then the lamp was put into a quartz sleeve and immersed within the photoreactor.

**2.4.2. Procedures and Analyses.** Photocatalytic activity of GR/TiO<sub>2</sub> composites was estimated by measuring the degradation percent of 2,4-D in an anoxic aqueous solution. The concentration of 2,4-D was from 50 mg L<sup>-1</sup>. The used amount of catalyst was 0.8 g/L; the GR/TiO<sub>2</sub> suspension was put into nitrogen from 0.5 to 2 hours before the reaction to drive part of dissolved oxygen of the reaction liquid and to ensure

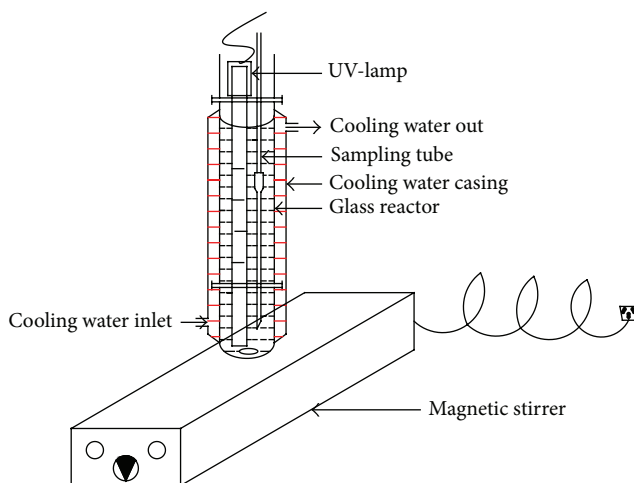


FIGURE 2: Schematic diagram of photoreactor set-up for 2,4-D degradation in anoxic water.

the establishment of adsorption-desorption equilibrium. The reaction time was 6–15 h.

The samples of 2,4-D photocatalytic degradation were taken out at interval. The solutions were filtered through a 0.45  $\mu$ m membrane filter. 2,4-D concentrations were measured using a high-performance liquid chromatograph (HPLC, Agilent 1200) equipped with an Agilent ZORBAX SB-C18 column (stainless steel 150 \* 4.6 mm) and a UV detector. A solution of MeOH/0.1% phosphate acid (60 : 40 V/V) was used as mobile phase. The mobile phase was filtered and sonicated in order to remove dissolved gas; the flow rate of the mobile phase for the analysis was kept at 1 mL/min under 10.7 MPa pressure and column temperature of 303 K using  $\lambda = 283$  nm for UV detection. Aliquots of 20  $\mu$ L were injected manually into the HPLC to determine the concentration of 2,4-D. Reagent grade standards were used to calibrate the HPLC.

The degradation efficiency (DE) was calculated as follows:

$$DE\% = 100 * \frac{(C_0 - C)}{C_0}, \quad (1)$$

where  $C_0$  and  $C$  are 2,4-D solution concentrations at time  $t = 0$  and any time, respectively. ( $C_0$  and  $C$  are the initial and any time concentrations of solute (mg/L), resp.)

The concentrations of Cl<sup>-</sup> ion were measured with an ion chromatograph (Dionex ICS-2500) equipped with an electrical conductivity detector (ECD), on an anionic exchange column (Ion Pack AS18, 2 \* 250 mm). Aliquots of 20  $\mu$ L were injected into the IC and carried with a mobile phase containing 1.7 mmol/L NaHCO<sub>3</sub> + 1.8 mmol/L Na<sub>2</sub>CO<sub>3</sub> solution with a flow rate of 0.25 mL·min<sup>-1</sup>.

The intermediates products of 2,4-D degradation were identified by HPLC/MS/MS (Agilent 6538 Q-TOF System) equipped with an ESI source. As for the HPLC condition in HPLC/MS/MS testing, MeOH : 0.1% methanoic acid = 70 : 30 was used as mobile phase and flow rate was set to 0.2 mL·min<sup>-1</sup> without a separation column. Full scale MS

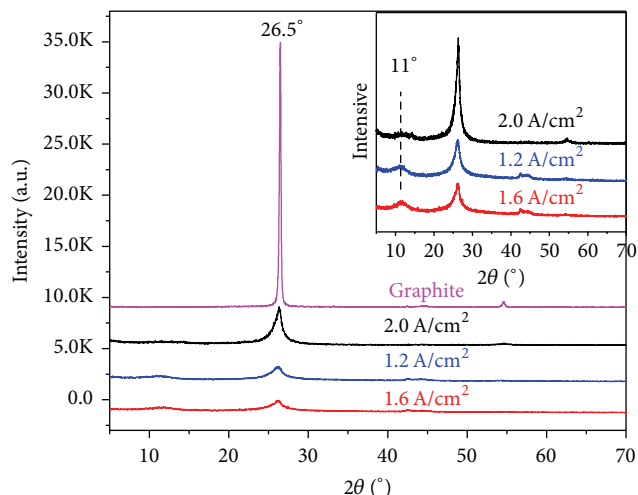


FIGURE 3: XRD spectra of graphite and EGR electrochemical stripping at different current density.

spectra in both negative modes in the mass range between 50 and 500  $m/z$  were recorded.

The DO concentration of the reaction liquid during photocatalytic reaction was determined by using dissolved oxygen meter (HQ30D, HACH, USA).

### 3. Results and Discussion

**3.1. The Influence of Different Current Density on the Graphite Electrochemical Stripping.** Figure 3 showed XRD spectra of EGR prepared by graphite electrochemical stripping when  $H_2SO_4$  was used as electrolyte, and current density was  $1.2 A/cm^2$ ,  $1.6 A/cm^2$ , and  $2.0 A/cm^2$ , respectively, and electrolyte was vacuum dried at  $50^\circ C$  for 24 h. It could be seen from Figure 3 that a sharp diffraction peak at  $26.5^\circ$  was observed in the original graphite XRD spectrum corresponding to the layer spacing which was 0.334 nm of graphite [17, 18].

In the process of electrochemical stripping of graphite, the sharp diffraction peak at  $26.5^\circ$  was decreased when the current density was  $1.2 A/cm^2$ , and a new peak at about  $11^\circ$  corresponding to the peak of graphite oxide [15] was produced; the diffraction peak at  $26.5^\circ$  became more smooth when current density was increased to  $1.6 A/cm^2$ ; when the current density was up to  $2.0 A/cm^2$ , diffraction peak at  $26.5^\circ$  became sharp, but the oxide diffraction peak was smoother. Current energy maybe has the dual role of improvement and inhibition during graphite electrochemical stripping process. When the current density was larger, it would make graphite surface oxidation but did not change graphite structure between the layers; then inducing the anion of electrolyte did not embed in graphite layers effectively, so it was not conducive to the layer spacing increases; thus lead to the stripping effect was not ideal. The XRD characterization results showed that when  $H_2SO_4$  was used as electrolyte and the current density was  $1.6 A/cm^2$ , the as-prepared graphene product had good characteristics of graphene.

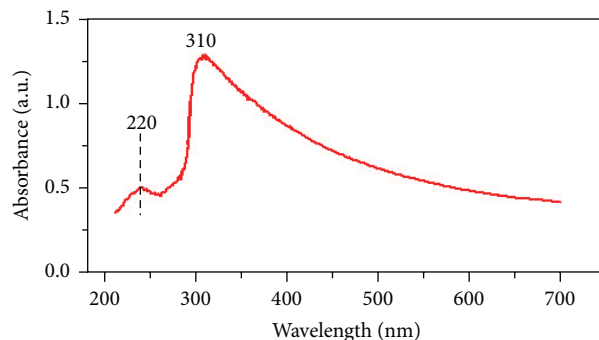


FIGURE 4: UV-Vis spectra of graphene.

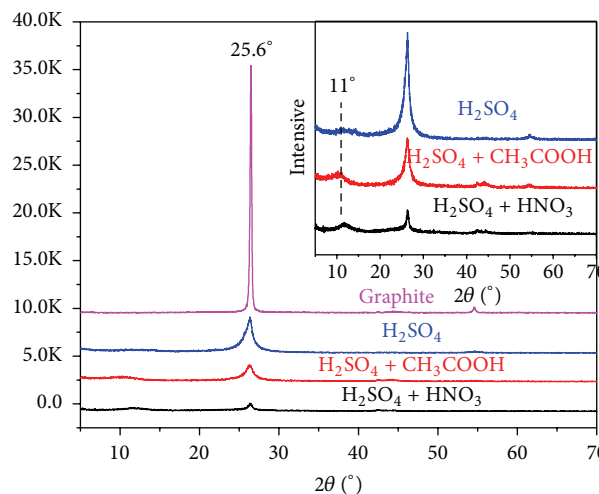


FIGURE 5: XRD spectra of graphite and EGR electrochemical stripping at different acid dopant.

After ultrasonic dispersion for 30 min, the UV-Vis absorbance characteristics of graphene prepared under the current density were  $1.6 A/cm^2$  which were shown in Figure 4. It could be seen from Figure 4 that the as-prepared graphene had a weaker absorption peak near 220 nm which was caused by  $n-\pi^*$  electron transition of C=O bond and had a strong absorption peak near 310 nm which was caused by  $\pi-\pi^*$  electron transition of C=C bond [19].

The results showed that there were traces of graphene oxide generated in the electrochemical stripping process and consistent with the characteristic results of XRD. This may be caused by the oxidation of part graphite surface at the beginning of the reaction and expand graphite layers; expanding graphite is easier to peel off under the coupling condition of ultrasonic and change voltage during electrochemical stripping.

**3.2. The Influence of Different Acid Dopant on Graphite Electrochemical Stripping.** Figure 5 showed XRD spectra of EGR prepared by graphite electrochemical stripping when current density was  $1.6 A/cm^2$ ,  $H_2SO_4 + HNO_3$  or  $H_2SO_4 + CH_3COOH$  was used as electrolyte, and electrolyte was vacuum dried at  $50^\circ C$ . It could be seen from Figure 5 that the diffraction peak of the as-prepared EGR was wider at

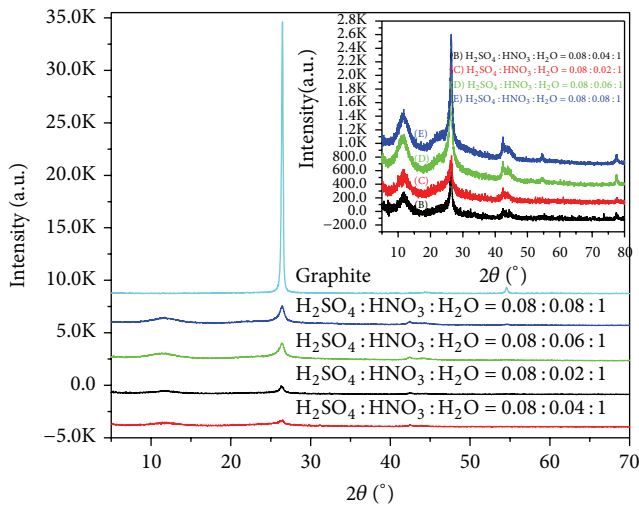


FIGURE 6: XRD spectra of graphite and graphene for different nitric acid doping ratio.

26.5° and was more obvious at about 11° when electrolyte solution was added to inorganic acid. In the process of electrolysis, the gradient force was produced by the anion in electrolyte under the action of electric field, which made the anion able to fully type graphite layer, and the layer spacing increases and weakens the graphite layer of interatomic forces greatly. The oxidation performance of HNO<sub>3</sub> was stronger than CH<sub>3</sub>COOH, and oxide graphite layer could change the surface structure of graphite layer and therefore increased the layers distance effectively. The XRD characterization results showed that when H<sub>2</sub>SO<sub>4</sub> was used as electrolyte, HNO<sub>3</sub> was used as electrolyte dopant, and the current density was 1.6 A/cm<sup>2</sup>, the as-prepared graphene product had good characteristics of graphene structure.

**3.3. The Effect of Nitric Acid Different Doped Ratio on Graphite Electrochemical Stripping.** Figure 6 showed XRD spectra of EGR prepared by graphite electrochemical stripping when current density was 1.6 A/cm<sup>2</sup>, the mixture of H<sub>2</sub>SO<sub>4</sub> and HNO<sub>3</sub> was used as electrolyte and H<sub>2</sub>SO<sub>4</sub>:HNO<sub>3</sub>:H<sub>2</sub>O = 0.08:0.02:1(V/V), H<sub>2</sub>SO<sub>4</sub>:HNO<sub>3</sub>:H<sub>2</sub>O = 0.08:0.04:1(V/V), H<sub>2</sub>SO<sub>4</sub>:HNO<sub>3</sub>:H<sub>2</sub>O = 0.08:0.06:1(V/V), and H<sub>2</sub>SO<sub>4</sub>:HNO<sub>3</sub>:H<sub>2</sub>O = 0.08:0.08:1(V/V), respectively, and the electrolytes were vacuum dried at 50°C for 24 hours. It could be seen from Figure 6 that the diffraction peak of the as-prepared EGR was wider at 26.5° and was more obvious at about 11° when electrolyte solution was added to inorganic acid. Figure 6 indicated that the diffraction peak at 26.5° is widest when the doping ratio of HNO<sub>3</sub>:H<sub>2</sub>O was 0.04, and diffraction peak was more acute when the doping ratio was 0.02, 0.06, or 0.08. The results showed that when amount of HNO<sub>3</sub> was doped in electrolyte, it could promote the electrochemical oxidation of graphite layers, resulting in graphite inflation, thus to further facilitate the electrochemical stripping of graphite. When the doping ratio of HNO<sub>3</sub>:H<sub>2</sub>O was too low, graphite layer could not be fully oxidized, which may lead to difficulty in separation of graphite layer. If the doping ratio of HNO<sub>3</sub> was too high,

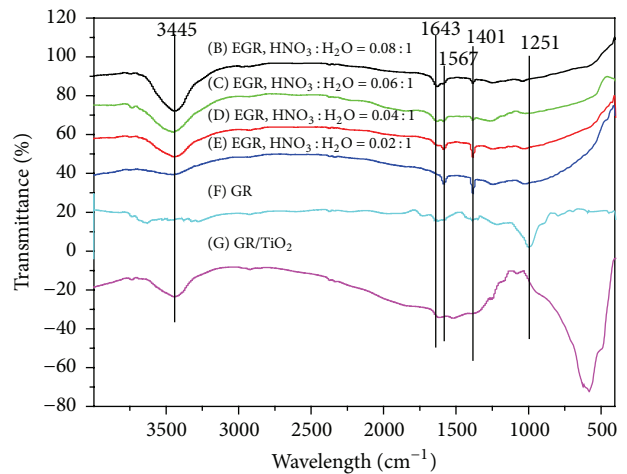


FIGURE 7: FTIR spectra of EGR, GR, and GR/TiO<sub>2</sub>.

it would result in making the oxidation of electrolyte too strong, thus reducing adsorption of electrolyte ion to graphite layer surface and going against the electrochemical stripping of graphite. The XRD characterization results showed that when the current density was 1.6 A/cm<sup>2</sup> and the doping ratio of HNO<sub>3</sub>:H<sub>2</sub>O was 0.02:1(V/V) and 0.04:1(V/V), the as-prepared graphene product had good characteristics of graphene structure.

Figure 7((B), (C), (D), and (E)) was the FTIR spectra of EGR prepared by graphite electrochemical stripping when current density was 1.6 A/cm<sup>2</sup>, and the mixture whose composition was H<sub>2</sub>SO<sub>4</sub>:HNO<sub>3</sub>:H<sub>2</sub>O = 0.08:0.02:1(V/V), H<sub>2</sub>SO<sub>4</sub>:HNO<sub>3</sub>:H<sub>2</sub>O = 0.08:0.04:1(V/V), H<sub>2</sub>SO<sub>4</sub>:HNO<sub>3</sub>:H<sub>2</sub>O = 0.08:0.06:1(V/V), and H<sub>2</sub>SO<sub>4</sub>:HNO<sub>3</sub>:H<sub>2</sub>O = 0.08:0.08:1(V/V), respectively, was used as electrolytes. It could be seen from the spectra that the as-prepared EGR had the following main characteristic absorption peaks: carbonyl (C=O) stretching vibration peak of the residual COOH groups 1720~1740 cm<sup>-1</sup>, 1251 cm<sup>-1</sup>, and 1024 cm<sup>-1</sup> was stretching vibration peak of C-OH and C-O-C, respectively [20, 21]; there was absorption peak near 3445 cm<sup>-1</sup> that belongs to the OH absorption peak; the absorption peak intensity of 3445 cm<sup>-1</sup>, 1643 cm<sup>-1</sup>, 1251 cm<sup>-1</sup>, and 1024 cm<sup>-1</sup> was obviously decreased with the decrease of HNO<sub>3</sub> content in the electrolyte; the peak located at 1643 cm<sup>-1</sup> was graphene peculiar stretching vibration. The results showed that the as-prepared EGR contains hydroxyl group, carboxyl group, and C-O-C and others contain oxygen groups. The characterization results of FTIR indicated that when current density was 1.6 A/cm<sup>2</sup> and the doping ratio of HNO<sub>3</sub>:H<sub>2</sub>O was 0.02:1(V/V) and 0.04:1(V/V), the product prepared by electrochemical stripping graphite had good properties of graphene.

**3.4. The Influence of High Temperature Crystallization in Hydrogen Atmosphere on EGR Reduction and TiO<sub>2</sub> Crystal Type.** Figure 7((F) and (G)) is about FTIR spectrum of GR and GR/TiO<sub>2</sub>, respectively. It could be seen from those figures that peak intensity of EGR located at 3445 cm<sup>-1</sup>, 1725 cm<sup>-1</sup>, 1251 cm<sup>-1</sup>, and 1024 cm<sup>-1</sup> was decreased significantly after

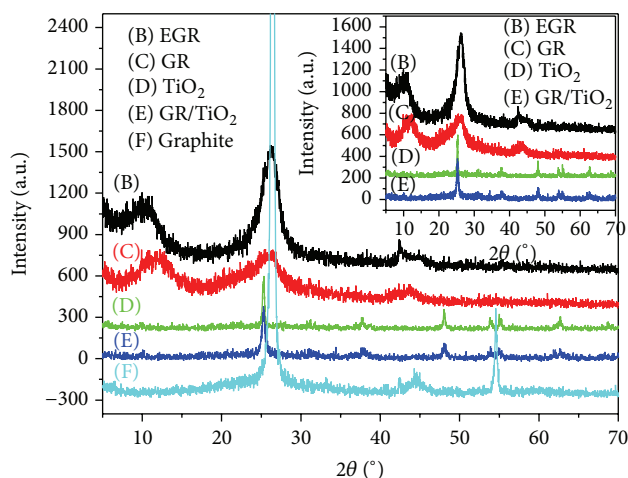


FIGURE 8: XRD spectra of EGR, GR, TiO<sub>2</sub>, GR/TiO<sub>2</sub>, and graphite.

high temperature crystallization in hydrogen atmosphere. In addition, a typical vibration peak of graphene structure appeared near  $1643\text{ cm}^{-1}$  [22]. The results showed that the  $\pi$  bond in the structure of GR had been restored. The FTIR spectra of GR/TiO<sub>2</sub> in Figure 7(G) indicated that there were absorption peaks located near  $3445\text{ cm}^{-1}$ ,  $1643\text{ cm}^{-1}$  and  $580\text{ cm}^{-1}$ , and  $1643\text{ cm}^{-1}$  corresponding to the skeleton vibration peak of graphene and the absorption peak near  $580\text{ cm}^{-1}$  corresponding to the stretching vibration of Ti-O-Ti in crystal TiO<sub>2</sub>. The absorption peak located near  $580\text{ cm}^{-1}$  was significantly widened after EGE and TiO<sub>2</sub> reduction crystallization; it was shown that the combination of GR and TiO<sub>2</sub> was stable, and the Ti-O-C bond was formed [12].

Figure 8 showed the XRD spectra of EGR, GR, TiO<sub>2</sub>, GR/TiO<sub>2</sub>, and graphite. The XRD patterns of EGR (Figure 8(B)) and GR (Figure 8(C)) revealed that the peak for EGR at  $10^\circ$  shifted to  $\sim 12^\circ$  and peak shape width; in addition, the strength of the peak at  $26.3^\circ$  was decreased obviously, which provides evidence of the reduction of part of EGR to GR (Figure 8(C)). The peak type of GR/TiO<sub>2</sub> (Figure 8(E)) is similar to anatase type TiO<sub>2</sub> (Figure 8(D)), which may be due to the too small content of GR in GR/TiO<sub>2</sub>, or GR combined with TiO<sub>2</sub>, and formed the Ti-O-C bond; the characterization results were similar to those of FTIR.

### 3.5. The Physicochemical Properties of GR and GR/TiO<sub>2</sub>.

Figure 9 showed the SEM images of GR and GR/TiO<sub>2</sub> composites. The SEM images of GR prepared by electrochemical stripping and high temperature heat reduction in hydrogen atmosphere method were shown in Figures 9(a) and 9(b). It could be seen from Figures 9(a) and 9(b) that the surface morphology of the as-prepared GR was folded lamellar structure, and its thickness varies from 0.7 nm to a few nanometers. This may be because graphene had strong surface energy which could make a micro distortion when two-dimensional crystal turned into three-dimensional crystal. Figures 9(c) and 9(d) showed the SEM images of GR/TiO<sub>2</sub> composites nanomaterial; the TiO<sub>2</sub> spherical nanoparticles were found to be deposited on GR and also intercalated in GR sheets.

Figure 10 showed the TEM images of GR and GR/TiO<sub>2</sub> composites. It could also be seen from Figure 10(a) that the surface morphology of the as-prepared GR was folded lamellar structure, and its thickness varies from 0.7 nm to a few nanometers. TiO<sub>2</sub> particles appear in spherical shape whose particles size was about 40–80 nm and deposited on the graphene lamellar surface. These results prove that the TiO<sub>2</sub> spherical nanoparticles were found to be deposited on GR and intercalated in the GR sheets with the bond of Ti-O-C.

The GR doping amount had great influence on the specific surface area of GR/TiO<sub>2</sub> composite nanomaterials. The results shown in Table I indicated that the TiO<sub>2</sub> particles were mesoporous structure and the specific surface area ( $S_{\text{BET}}$ ) of TiO<sub>2</sub> prepared by the same sol-gel and high temperature crystallization in hydrogen atmosphere was  $85.4\text{ m}^2\cdot\text{g}^{-1}$ . When the GR load contents increased from 0% to 1.5%, its corresponding  $S_{\text{BET}}$  ranged from  $85.4\text{ m}^2\cdot\text{g}^{-1}$  to  $192.7\text{ m}^2\cdot\text{g}^{-1}$ . While the GR load contents increased from 1.5% to 2%,  $S_{\text{BET}}$  of GR/TiO<sub>2</sub> decreased from  $192.7\text{ m}^2\cdot\text{g}^{-1}$  to  $83.6\text{ m}^2\cdot\text{g}^{-1}$ . It turned out that GR may jam the pore inside after being loaded and reduced  $S_{\text{BET}}$  of GR/TiO<sub>2</sub> composite nanomaterials.

### 3.6. Photocatalytic Activity of GR/TiO<sub>2</sub>

#### Composite Nanomaterials

**3.6.1. The Effect of GR Doping Amount on GR/TiO<sub>2</sub> Photocatalytic Activity.** 2,4-D photocatalytic degradation efficiency by using TiO<sub>2</sub> and GR/TiO<sub>2</sub> as photocatalyst was shown in Figure 11. It can be seen from Figure 11 that the GR/TiO<sub>2</sub> exhibited higher photocatalytic activity than P25-TiO<sub>2</sub>. Under the same photocatalytic reaction condition, the degradation rate of 2,4-D was 80.73% and above 90% by using P25-TiO<sub>2</sub> and GR/TiO<sub>2</sub> as photocatalyst after 10 h, respectively. The results showed that the as-prepared GR had good electronic transmission performance; after being combined with TiO<sub>2</sub>, GR can extend recombining time of photoproduction electrons and holes and therefore improve the efficiency of quantization. GR doping amount had a great influence on the catalytic performance of GR/TiO<sub>2</sub>. Under the same photocatalytic reaction condition, the degradation rate of 2,4-D was 90.91%, 96.45%, 93.45%, and 86.45% by using 0.01 GR/TiO<sub>2</sub>, 0.015 GR/TiO<sub>2</sub>, 0.02 GR/TiO<sub>2</sub>, and 0.03 GR/TiO<sub>2</sub> as photocatalyst after 10 h, respectively. The experimental results showed that the adsorption capacity of TiO<sub>2</sub> could be improved after doping appropriate amount of GR to TiO<sub>2</sub>, and the electronic migration pathway would be changed and therefore can improve the efficiency of quantization; on the other hand, if the doping amount of GR was too high, the light distribution would be restrained and it will be disadvantageous to the production of photoproduction electronic, thereby resulting in the decrease of GR/TiO<sub>2</sub> photocatalytic activity.

**3.6.2. The Influence of Initial DO Concentration on the Degradation of 2,4-D.** The influence of initial concentrations of DO on the degradation of 2,4-D was studied from 9.14 mg/L to 1.16 mg/L. Figure 12 showed the degradation percentage of 2,4-D and the change of the DO concentration during

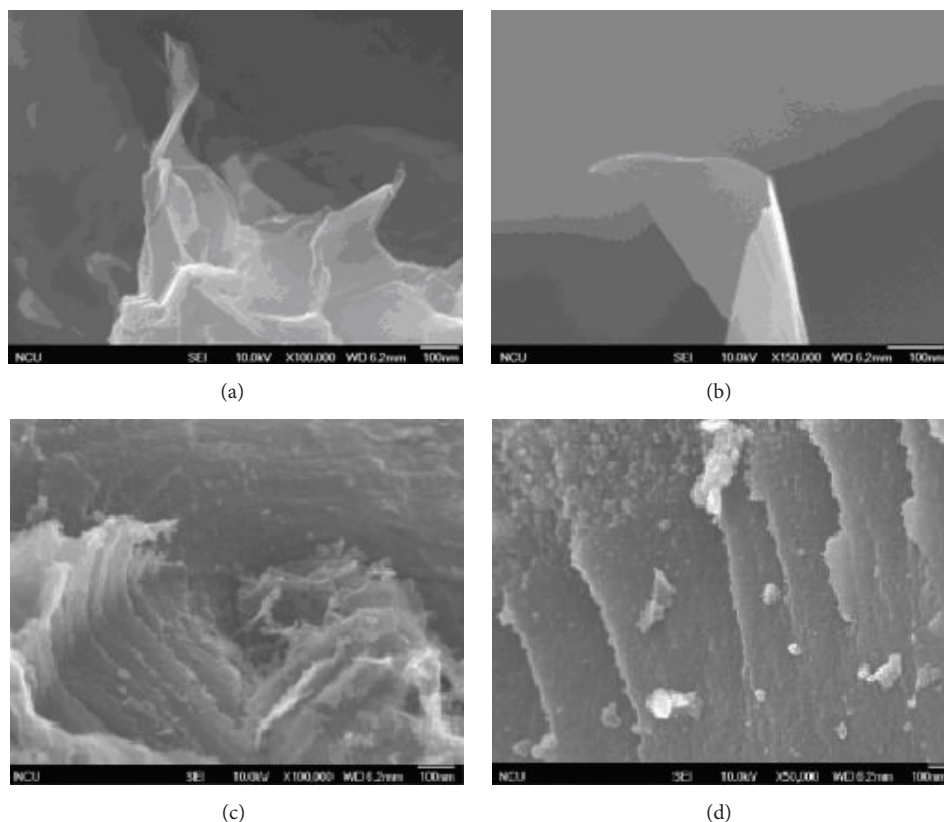


FIGURE 9: SEM patterns of the GR and GR/TiO<sub>2</sub> (GR: (a), (b); GR/TiO<sub>2</sub>: (c), (d)).

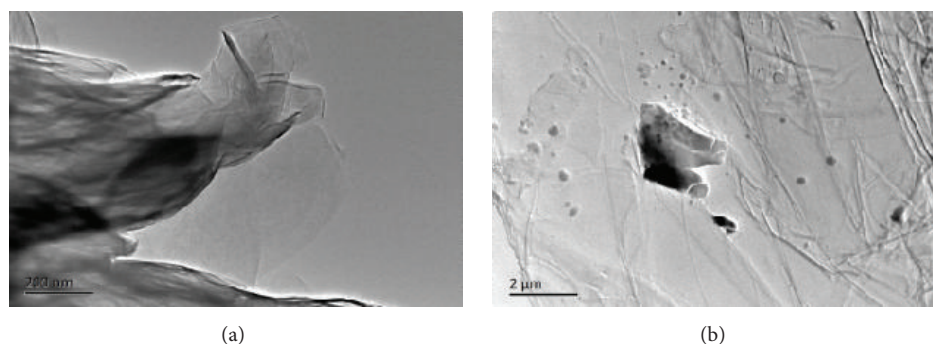


FIGURE 10: TEM images of the GR and GR/TiO<sub>2</sub> (GR: (a), GR/TiO<sub>2</sub>: (b)).

reaction processes in anoxic reactor (Figure 2) under the condition of 0.015 GR/TiO<sub>2</sub> photocatalyst dose equal to 0.8 g/L, pH was 7.0, and initial concentration of 2,4-D was 50 mg/L. The results indicated that the higher the initial concentration of DO, the faster the 2,4-D degradation in anoxic water environment. When the initial concentration of DO was 9.14 mg/L, 2.2 mg/L, and 1.16 mg/L, the gradation percentage was 77%, 60%, and 49% after 8 h, respectively; at the same time, concentration of DO was decreased to 5.2 mg/L (Figure 12(C)), 0.92 mg/L (Figure 12(E)), and 0.5 mg/L (Figure 11(G)), respectively. After 28 h (Figure 12(B)), 30 h (Figure 12(D)), and 41 h (Figure 12(F)), 2,4-D was degraded completely.

**3.6.3. Catalyst Lifetime Assessment.** The catalyst lifetime was assessed according to the degradation percentage of 2,4-D by the repeatedly used GR/TiO<sub>2</sub> composite nanomaterials. GR/TiO<sub>2</sub> separated from reaction liquid after the end of photocatalytic reaction each time by the method of placement for 12 hours and poured out of the upper cleared liquid, with then drying in an oven for 4 h in the temperature of 110°C calcination in the muffle furnace at 300°C for 4 hours. The photocatalytic reaction experiment continues on the same conditions for nine times; the results of Figure 13 showed that the degradation percentage of 2,4-D was less than 5% after the GR/TiO<sub>2</sub> used for nine times. The outcomes indicated that

TABLE 1: Specific surface area of TiO<sub>2</sub> and GR/TiO<sub>2</sub>.

Sample	TiO <sub>2</sub>	0.01 GR/TiO <sub>2</sub>	0.015 GR/TiO <sub>2</sub>	0.02 GR/TiO <sub>2</sub>	0.03 GR/TiO <sub>2</sub>
$S_{BET}/(m^2 \cdot g^{-1})$	85.4	131.4	192.7	83.6	80.4

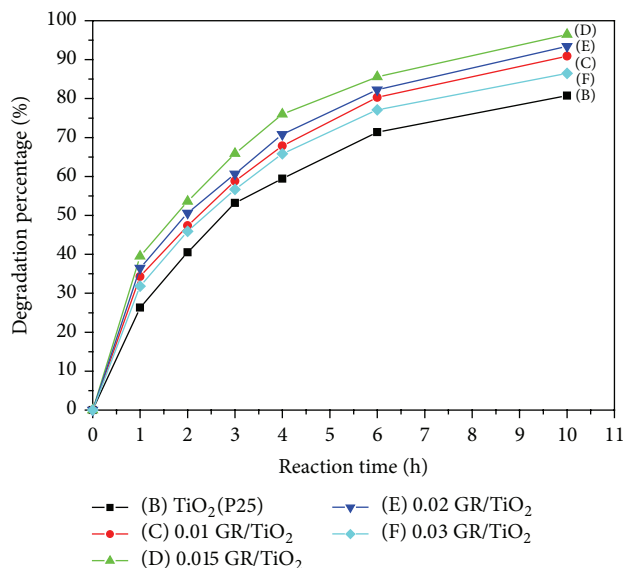
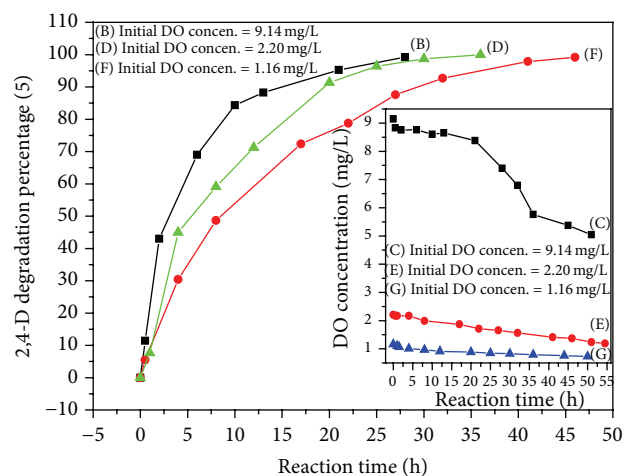
FIGURE 11: The effect of GR doping amount on the photocatalytic activity of GR/TiO<sub>2</sub>.

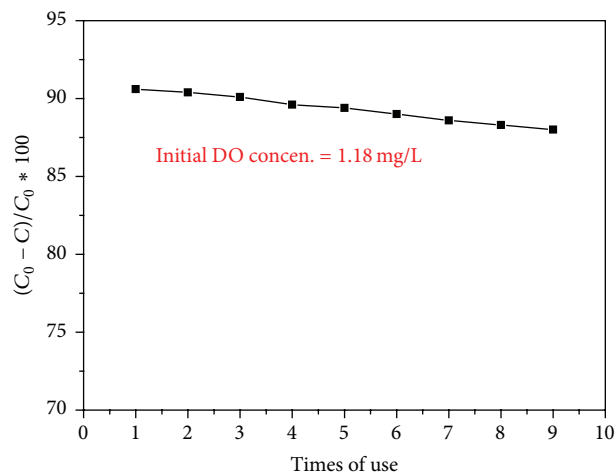
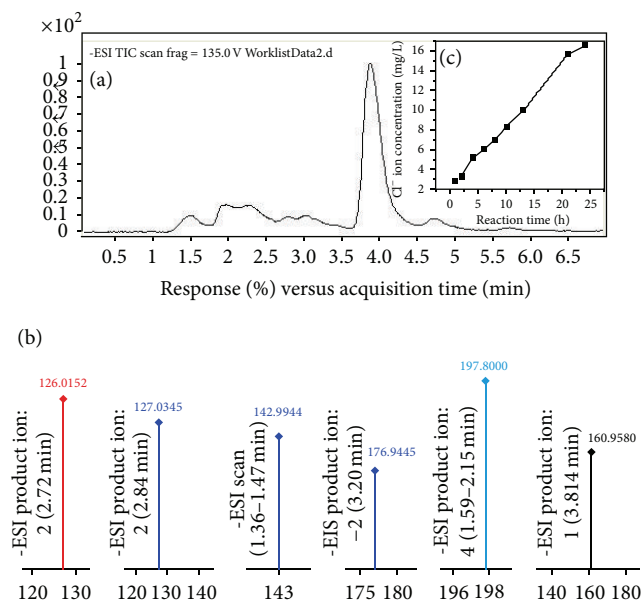
FIGURE 12: The influence of initial concentrations of DO on the degradation of 2,4-D.

the as-prepared GR/TiO<sub>2</sub> could be used repeatedly, and its photocatalytic activity kept little change.

### 3.6.4. Proposed Photocatalytic Degradation

#### Mechanism of 2,4-D

(1) *2,4-D Photocatalytic Degradation Intermediate Analysis.* The intermediate products of 2,4-D photocatalytic were degraded by using 0.015 GR/TiO<sub>2</sub> as photocatalyst and the reaction time was 10 h which was tested by HPLC/MS/MS

FIGURE 13: The effect of use times of GR/TiO<sub>2</sub> on the degradation of 2,4-D.FIGURE 14: The HPLC/MS/MS and IC analysis sketch of 2,4-D degradation intermediate products ((a) TIC; (b) molecular ion peak; (c) Cl<sup>-</sup> ion).

and IC. The analysis results were shown in Figure 14 and Table 2. Figure 14(a) showed the total ion current (TIC); it indicated that there were a number of intermediates generated during 2,4-D photocatalytic degradation. The analysis results of TIC by MS/MS were shown in Figure 14(b); those results showed that there were several molecular ion peaks such as 126.0152, 127.0345, 142.9944, 160.9580, 176.9445, and 197.5000, detected at 2.72 min, 2.84 min, 1.36~1.47 min,



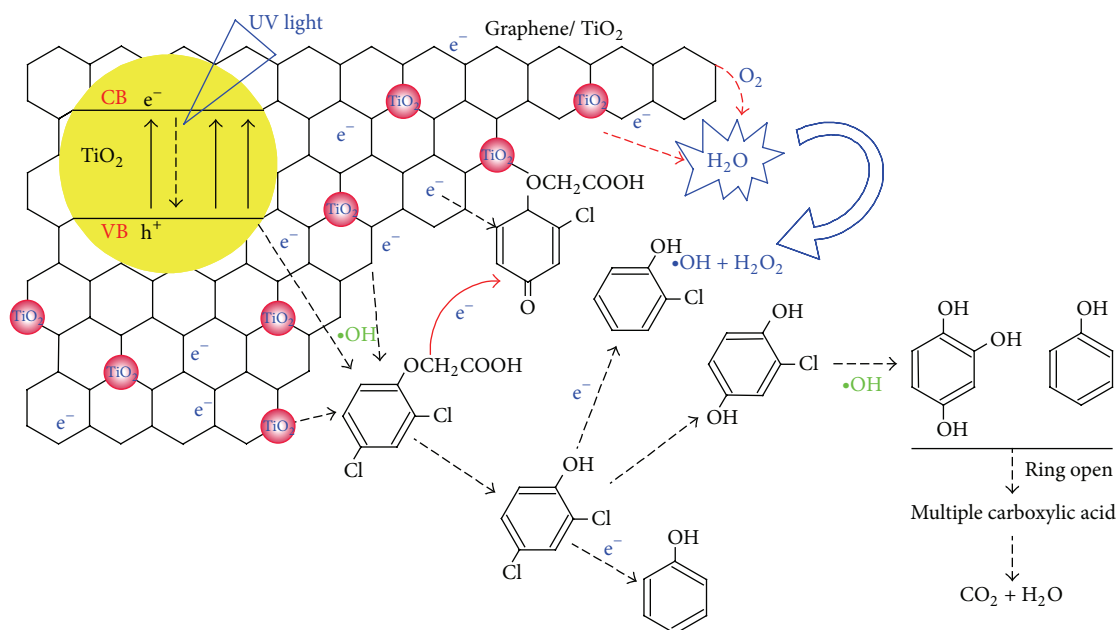


FIGURE 15: Possible degradation mechanism of 2,4-D in anoxic water environment.

3.814 min, 3.20 min, and 1.59~2.15 min in TIC, respectively. The possible molecular formula and structural formula were deduced in Table 2; the results of Table 2 illustrated that some oxidative degradation products such as dichlorophenol and dichlorobenzene hydroquinone were produced, and some reductive degradation products such as hydroxyhydroquinone and chlorophenol chlorine diphenol were produced. Figure 14(c) showed  $\text{Cl}^-$  concentration produced in the process of photocatalytic reaction; the determination data showed that the longer the reaction time, the greater the concentration of chloride ion; it also indicated that both oxidation and reductive reaction happened.

(2) *Proposed Photocatalytic Degradation Mechanism of 2,4-D.* The testing results of HPLC/MS/MS and IC indicate that two kinds of intermediates were detected, that is, chlorophenol and polyhydroxylated intermediates. In the presence of 1.0~2.0 mg/L DO and light, photoproduction electronic migrated through graphene and reacted with DO to produce hydroxyl radicals ( $\cdot\text{OH}$ ), resulting in oxidizing degradation of 2,4-D; the bond of hydroxyacetic acid in 2,4-dichlorophenoxyacetic acid was broken first, and 2,4-dichlorophenol (2,4-DCP) was formed. The hydroxyl radicals belong to electrophilic attack; the reaction took place preferentially at *ortho*-position and *para*-position of hydroxyl in 2,4-DCP molecule, owing to those positions with higher electron density. Because the *ortho*-positions were vacant, the addition of hydroxyl group to the benzene ring would result in the formation of polyhydroxylated intermediates. On the other hand, part of the photoproduction electronic direct attacked chlorine in benzene ring of 2,4-D and its intermediate products, resulting in dechlorination reduction degradation of 2,4-D; when the DO concentration of the reaction liquid reduced to about 0.5 mg/L and, then, remained the same, photoproduction electronic did not combine with  $\text{O}_2$  but attacked 2,4-D

molecules directly and made the 2,4-D molecules reductive dechlorination. According to the above-mentioned results, possible degradation mechanism of 2,4-D was proposed as shown in Figure 15.

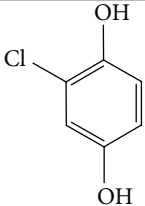
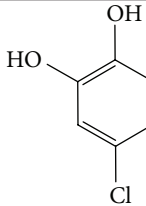
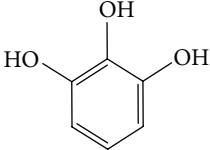
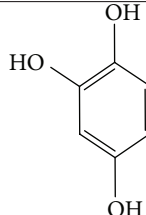
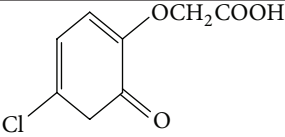
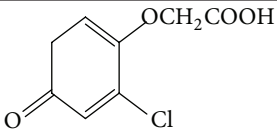
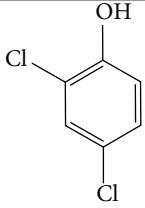
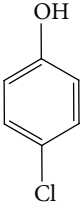
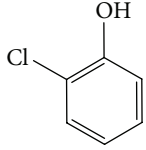
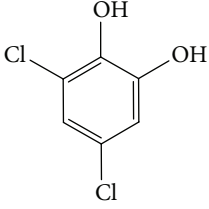
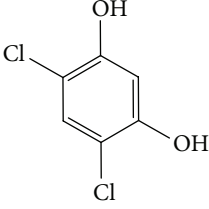
#### 4. Conclusion

The graphene (GR) was prepared by an improved electrochemical stripping method using a high-purity graphite rod as raw material and high temperature heat reduction under hydrogen atmosphere, and the electrochemical stripping conditions on the influence of the physical and chemical properties of the as-prepared GR were studied detailedly. The results showed that when the current density was  $1.6 \text{ A/cm}^2$ , the mixture of  $\text{H}_2\text{SO}_4 : \text{HNO}_3 : \text{H}_2\text{O} = 0.08 : 0.02 : 1(\text{V/V})$  and  $\text{H}_2\text{SO}_4 : \text{HNO}_3 : \text{H}_2\text{O} = 0.08 : 0.04 : 1(\text{V/V})$  was used as electrolyte under the coupling condition of ultrasonic and change voltage; the stripping product from graphite had good properties of graphene.

The GR/ $\text{TiO}_2$  composite nanomaterials were manufactured by the method of sol-gel and high temperature crystallization in hydrogen atmosphere using butyl titanate and electrolysis graphene as precursors. The microstructure and morphology of samples were characterized by XRD, FTIR, SEM, TEM, BET, and so forth. The results proved that the  $\text{TiO}_2$  spherical nanoparticles were found to be deposited on GR and intercalated in the GR sheets with the bond of Ti-O-C.

The photocatalytic oxidation reduction characteristics of GR/ $\text{TiO}_2$  in anoxic water by using 2,4-D as goal pollutant were studied, and the possible degradation mechanism was discussed. The influence of graphene doping amount and initial concentration of dissolved oxygen on the degradation of 2,4-D was studied detailedly. The results showed that when the doping ratio of GR: $\text{TiO}_2$  was equal to 0.015,

TABLE 2: PHLC/MS/MS analysis results of 2,4-D degradation intermediate products.

Serial number	Ion peak	Peak time/min	Possible formulas	Possible structural formula	
1	142.9944	1.36~1.47	$C_6H_5ClO_2$		
2	126.0152	1.36~1.47	$C_6H_6O_3$		
3	197.8000	1.59~2.53	$C_8H_7ClO_4$		
4	160.9580	2.72	$C_6H_4Cl_2O$		
5	127.0385	2.84	$C_6H_5ClO$		
6	176.9045	3.20	$C_6H_4Cl_2O_2$		

the as-prepared GR/TiO<sub>2</sub> had good photocatalytic activity, and when initial DO concentration was from 1.16 mg/L to 2.2 mg/L, the degradation percentage could be attained 60% after 8 h and degraded completely after 40 h.

In the anoxic water environment, photoproduction electronic migrated through graphene and reacted with DO in the water to produce hydroxyl radicals ( $\cdot OH$ ), resulting in oxidizing degradation of 2,4-D; on the other hand, part of the photoproduction electronic direct attacked chlorine in benzene ring of 2,4-D and its intermediate products, resulting in dechlorination reduction degradation; when the DO concentration of the reaction liquid reduced to about 0.5 mg/L, photoproduction electronic did not react with O<sub>2</sub>

but attacked 2,4-D molecules directly and made the 2,4-D molecules reductive dechlorination.

### Competing Interests

The authors declare that they have no competing interests.

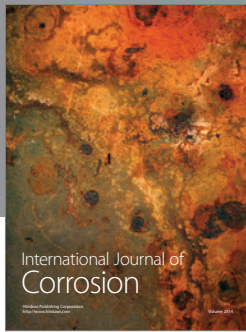
### Acknowledgments

The authors gratefully acknowledge the financial support of the Cultivation Fund of the Key Scientific and Technical Innovation Project, Ministry of Education of

China (no. 508057), the Scientific Research Foundation of Jiangxi Provincial Department of Education (GJJ10116), and the Scientific Research Foundation of Jiangxi Province (2010BSB03003).

## References

- [1] W. Li, Z. Wu, J. Wang, A. A. Elzatahry, and D. A. Zhao, "A perspective on mesoporous TiO<sub>2</sub> materials," *Chemistry of Materials*, vol. 26, no. 1, pp. 287–298, 2014.
- [2] W. Zhang, X.-X. Wang, and X.-Z. Fu, "Effect of platinum loading on lifetime of photogenerated charge carriers of TiO<sub>2</sub> studied by time-resolved photoconductivity," *Chemical Journal of Chinese Universities*, vol. 26, no. 10, pp. 1861–1864, 2005.
- [3] H. Zhang, L.-H. Guo, D. Wang, L. Zhao, and B. Wan, "Light-induced efficient molecular oxygen activation on a Cu(II)-grafted TiO<sub>2</sub>/graphene photocatalyst for phenol degradation," *ACS Applied Materials and Interfaces*, vol. 7, no. 3, pp. 1816–1823, 2015.
- [4] K. S. Novoselov, A. K. Geim, S. V. Morozov et al., "Electric field effect in atomically thin carbon films," *Science*, vol. 306, no. 5696, pp. 666–669, 2004.
- [5] S. Anandan, T. Narasinga Rao, M. Sathish, D. Rangappa, I. Honma, and M. Miyachi, "Superhydrophilic graphene-loaded TiO<sub>2</sub> thin film for self-cleaning applications," *ACS Applied Materials and Interfaces*, vol. 5, no. 1, pp. 207–212, 2013.
- [6] M. Cai, D. Thorpe, D. H. Adamson, and H. C. Schniepp, "Methods of graphite exfoliation," *Journal of Materials Chemistry*, vol. 22, no. 48, pp. 24992–25002, 2012.
- [7] L. Q. Wu, W. W. Li, P. Li et al., "Powder, paper and foam of few-layer graphene prepared in high yield by electrochemical intercalation exfoliation of expanded graphite," *Small*, vol. 10, no. 7, pp. 1421–1429, 2014.
- [8] W. N. Zhang, W. He, and X. L. Jing, "Preparation of a stable graphene dispersion with high concentration by ultrasound," *Journal of Physical Chemistry B*, vol. 114, no. 32, pp. 10368–10373, 2010.
- [9] P. Jacobson, B. Stöger, A. Garhofer et al., "Nickel carbide as a source of grain rotation in epitaxial graphene," *ACS Nano*, vol. 6, no. 4, pp. 3564–3572, 2012.
- [10] S. Hofmann, P. Braeuninger-Weimer, and R. S. Weatherup, "CVD-enabled graphene manufacture and technology," *Journal of Physical Chemistry Letters*, vol. 6, no. 14, pp. 2714–2721, 2015.
- [11] R. M. Jacobberger, R. Machhi, J. Wroblewski, B. Taylor, A. L. Gillian-Daniel, and M. S. Arnold, "Simple graphene synthesis via chemical vapor deposition," *Journal of Chemical Education*, vol. 92, no. 11, pp. 1903–1907, 2015.
- [12] Z. H. Zhang, L. D. Zhang, W. Li, A. S. Yu, and P. Y. Wu, "Carbon-coated mesoporous TiO<sub>2</sub> nanocrystals grown on graphene for lithium-ion batteries," *ACS Applied Materials and Interfaces*, vol. 7, no. 19, pp. 10395–10400, 2015.
- [13] W. S. Hummers Jr. and R. E. Offeman, "Preparation of graphitic oxide," *Journal of the American Chemical Society*, vol. 80, no. 6, p. 1339, 1958.
- [14] B. Subramanya and D. K. Bhat, "Novel eco-friendly synthesis of graphene directly from graphite using 2,2,6,6-tetramethylpiperidine 1-oxyl and study of its electrochemical properties," *Journal of Power Sources*, vol. 275, pp. 90–98, 2015.
- [15] C. F. Chang, Q. Du, and J. R. Chen, "RETRACTED: graphene sheets synthesized by ionic-liquid-assisted electrolysis for application in water purification," *Applied Surface Science*, vol. 264, pp. 329–334, 2013.
- [16] P. Khanra, T. Kuila, S. H. Bae, N. H. Kim, and J. H. Lee, "Electrochemically exfoliated graphene using 9-anthracene carboxylic acid for supercapacitor application," *Journal of Materials Chemistry*, vol. 22, no. 46, pp. 24403–24410, 2012.
- [17] S. Y. Toh, K. S. Loh, S. K. Kamarudin, and W. R. W. Daud, "Graphene production via electrochemical reduction of graphene oxide: synthesis and characterisation," *Chemical Engineering Journal*, vol. 251, pp. 422–434, 2014.
- [18] H.-L. Guo, X.-F. Wang, Q.-Y. Qian, F.-B. Wang, and X.-H. Xia, "A green approach to the synthesis of graphene nanosheets," *ACS Nano*, vol. 3, no. 9, pp. 2653–2659, 2009.
- [19] D. Li, M. B. Müller, S. Gilje, R. B. Kaner, and G. G. Wallace, "Processable aqueous dispersions of graphene nanosheets," *Nature Nanotechnology*, vol. 3, no. 2, pp. 101–105, 2008.
- [20] S. H. Yang, Y. Lin, X. F. Song, P. Zhang, and L. Gao, "Covalently coupled ultrafine H-TiO<sub>2</sub> nanocrystals/nitrogen-doped graphene hybrid materials for high-performance supercapacitor," *ACS Applied Materials and Interfaces*, vol. 7, no. 32, pp. 17884–17892, 2015.
- [21] S. Yang, X. Song, P. Zhang, J. Sun, and L. Gao, "Self-assembled  $\alpha$ -Fe<sub>2</sub>O<sub>3</sub> mesocrystals/graphene nanohybrid for enhanced electrochemical capacitors," *Small*, vol. 10, no. 11, pp. 2270–2279, 2014.
- [22] L.-Q. Peng, J.-H. Xie, C. Guo, and D. Zhang, "Review of characterization methods of graphene," *Journal of Functional Materials*, vol. 44, no. 21, pp. 3055–3059, 2013.



**Hindawi**

Submit your manuscripts at  
<http://www.hindawi.com>

